

Highly Effective Surface Passivation of PbSe Quantum Dots through Reaction with Molecular Chlorine

Wan Ki Bae,^{†,||} Jin Joo,^{⊥,||} Lazaro A. Padilha,[†] Jonghan Won,[‡] Doh C. Lee,[†] Qianglu Lin,[§] Weon-kyu Koh,[†] Hongmei Luo,[§] Victor I. Klimov,^{*,†} and Jeffrey M. Pietryga^{*,†}

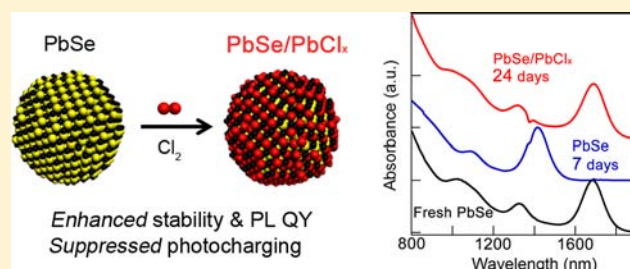
[†]Chemistry Division and [‡]Materials Science and Technology Division, Los Alamos National Laboratory, Los Alamos, New Mexico 87545, United States

[§]Department of Chemical Engineering, New Mexico State University, Las Cruces, New Mexico 88003, United States

[⊥]Department of Applied Chemistry, Kyungpook National University, Daegu 702-701, Korea

Supporting Information

ABSTRACT: PbSe nanocrystal quantum dots (NQDs) are a promising active material for a range of optoelectronic devices, including solar cells, high-sensitivity infrared (IR) photo-detectors, and IR-emitting diodes and lasers. However, device realization has been constrained by these NQDs' chemical instability toward oxidation, which leads to uncontrollable changes in optical and electronic properties. Here, we present a simple method to enhance the stability of PbSe NQDs against oxidation and to improve their optical properties through reaction with molecular chlorine. The chlorine molecules preferentially etch out surface Se ions and react with Pb ions to form a thin (1–2 monolayers) PbCl_x passivation layer which effectively prevents oxidation during long-term air exposure while passivating surface trap states to increase photoluminescence efficiency and decrease photocharging. Our method is simple, widely applicable to PbSe and PbS NQDs of a range of sizes, compatible with solution-based processes for fabricating NQD-based devices, and effective both in solution and in solid NQD films; thus, it is a practical protocol for facilitating advances over the full range of optoelectronic applications.



INTRODUCTION

Colloidal lead chalcogenide nanocrystal quantum dots (PbE NQDs, E = S, Se, and Te) have been extensively investigated as active materials for infrared- (IR-) emitting diodes,¹ lasers,² and IR-detectors.³ Their use has become increasingly widespread because they can be synthesized using relatively simple methods to exhibit bright, narrow emission at energies spanning a very wide range from the near- to mid-IR.^{4–9} Recently, these NQDs have garnered particularly intense attention among other IR NQDs because of their primary place in the development of next-generation NQD-based solar cells. This surge was inspired largely by reports of high carrier multiplication (CM) efficiencies in PbE NQDs.^{10–12} CM is a process in which absorption of a single high-energy photon can create more than one electron–hole pair within a NQD, and the potential for this phenomenon to increase the current in a solar cell has been verified in photocurrent measurements of real, functional PbSe NQD solar cells.¹³ In fact, to date all of the certified power conversion efficiency benchmarks for “quantum dot cells” are based on PbE NQDs.^{14–17}

Unfortunately, the development of all types of optoelectronic devices based on these materials has been hampered by instability toward oxidation under ambient conditions, particularly of PbTe⁸ and PbSe.¹⁸ For instance, despite the superior properties of PbSe, including higher bulk carrier

mobilities and greater measured CM efficiencies in NQDs,¹⁹ efforts to achieve higher efficiencies in quantum dot solar cells have focused solely on PbS because of its relatively higher stability. In addition to uncontrollable changes to the effective band gap and photoluminescence (PL) quantum yield (QY), oxidation of PbSe under ambient conditions can also affect the nature of surface trap states that can alter charge transport in NQD films²⁰ as well as participate in undesirable photocharging of the NQDs.^{21,22} Control over photocharging is particularly important because it can reduce PL QY, which is key for light-emitting diode and optical labeling applications,²³ and because of its relationship to CM. Photocharging is a competing process that interferes with both measurement¹¹ and device exploitation of CM; thus, its suppression is an important step toward necessary fundamental and applied advances in NQD-based solar cells.

In order to improve their optical properties as well as to enhance the chemical and photostability of PbSe NQDs, several approaches have been developed, including passivation of the NQD surface with thick, robust inorganic shells^{24,25} or by encapsulating NQD films in air-stable inorganic matrices (e.g., ZnO).²⁶ While these measures have achieved varying levels of

Received: October 3, 2012

Published: November 6, 2012

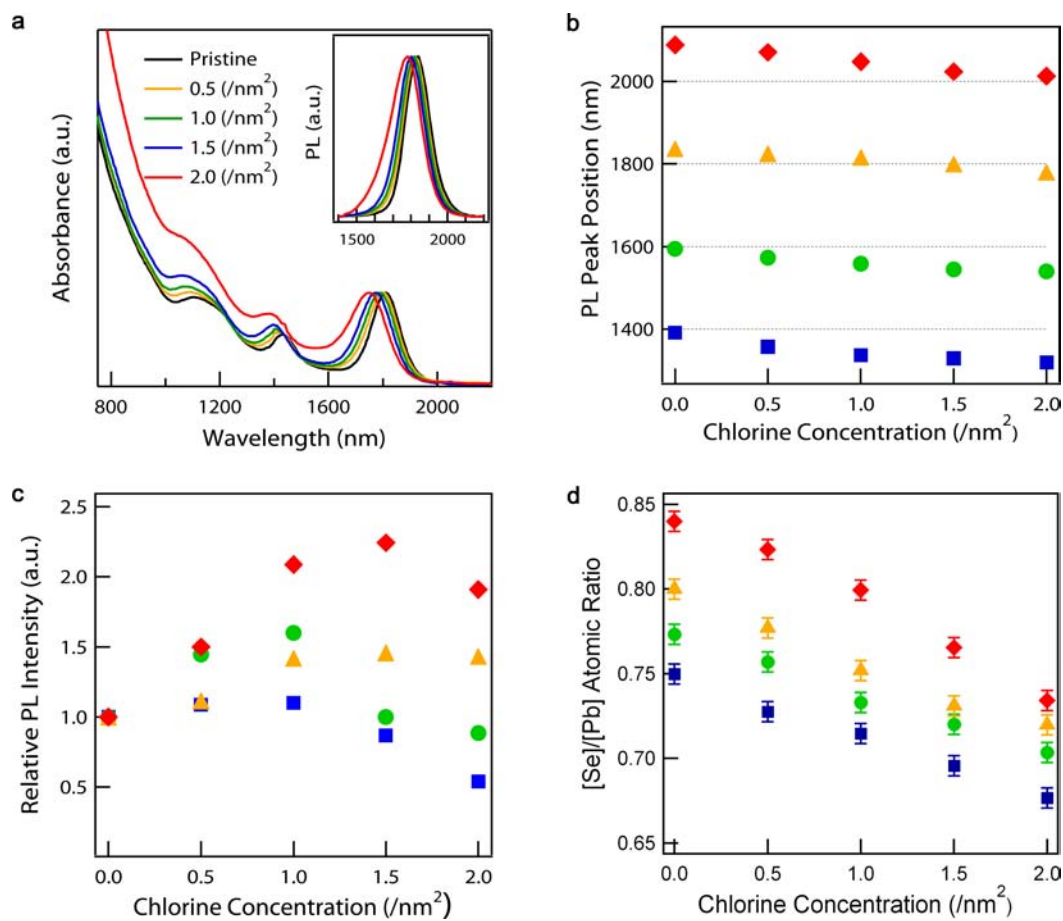


Figure 1. Spectral and chemical composition analyses on PbSe NQDs treated with Cl₂. (a) Normalized optical absorption and PL spectra (inset) of PbSe NQDs (diameter $d = 6.5$ nm) treated with different amounts of Cl₂. (b–d) PL peak wavelengths, PL QYs and Pb:Se atomic ratios of four samples of PbSe NQDs ($d = 3.9, 5.3, 6.5,$ and 7.9 nm denoted with squares, circles, triangles, and diamonds, respectively) as a function of Cl₂ concentration.

success, they result in a complex, heterostructured material in which the dynamics of charge carriers within individual NQDs and transport of carriers through an NQD film are fundamentally altered from those expected in a material based on pure PbSe NQDs. As this potentially tempers the specific advantages of PbSe NQDs, a better solution would be a simple method that engenders air-stability without drastically altering the structure or processability of the original NQDs.

Here, we present a simple and reproducible method to enhance the stability of PbSe or PbS NQDs against oxidation while reducing the effects of surface traps without drastic structural changes that can complicate device applications. This is accomplished by a solution-based postsynthetic treatment of the surface of PbSe NQDs with molecular chlorine (Cl₂). We observe that the Cl₂ preferentially etches surface Se atoms and reacts with Pb atoms to form a very thin, 1–2 atomic monolayer PbCl_x passivation layer that effectively prevents surface oxidation over time, in solution as well as in thin films, while enhancing PL QY and reducing detrimental effects due to photocharging. As such, chlorine treatment is a facile chemical means to enhance both the chemical stability and the optical properties of PbSe NQDs in a manner compatible with the solution-based processing methods that are a unique benefit of these nanomaterials.

RESULTS AND DISCUSSION

The motivation for exploring the treatment of lead chalcogenide NQDs with molecular chlorine was the observation that PbSe NQDs dispersed in chlorinated organic solvents (i.e., chloroform) generally exhibit higher PL intensity and better spectral stability against oxidation compared with those dispersed in, e.g., hexane or toluene (Figure S1). This raises the possibility that trace amounts of reactive chlorine-containing species that can naturally arise through the reaction of chlorinated organics with air and/or moisture (e.g., phosgene, HCl, Cl₂) might actually be beneficial. Preliminary studies in which PbSe NQDs were exposed to solutions containing chloride ion (Cl⁻) did not produce notable effects, although simple halide-ion exchange has been reported to be an effective way to remove long-chain ligands from lead chalcogenide NQDs.^{16,17} That being the case, we turned our attention to molecular chlorine (Cl₂), which is a convenient stand in for any type of oxidative Cl-containing species. Such strong oxidizing agents might be expected to react with ligands or surface atoms rather than simply replace surface ligands, as is case for the essentially inert Cl⁻ ion.

All chlorine treatments were carried out in solution phase at room temperature by slowly adding the desired amount of a 10 mM solution of Cl₂ in CCl₄ to a stirred sample of PbSe NQDs dispersed in toluene, and then isolating the NQDs by precipitation and redispersion in hexane. During the study,

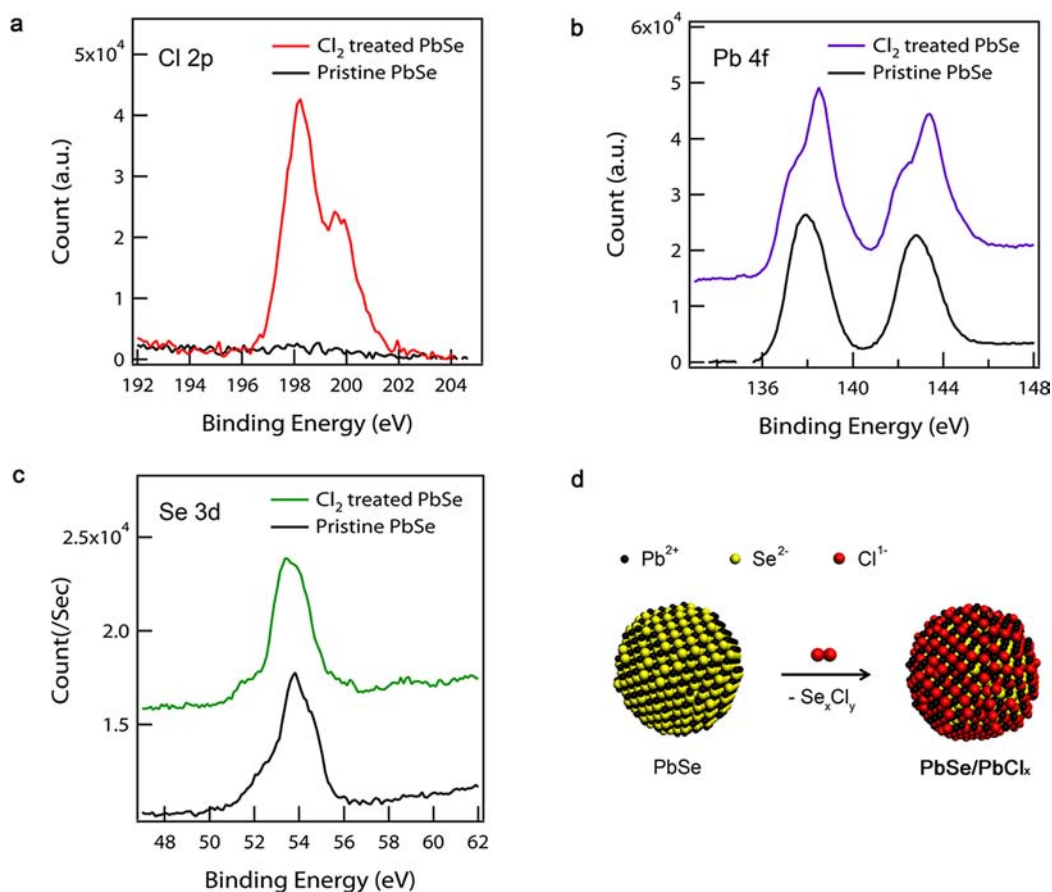


Figure 2. X-ray photoelectron spectroscopy of PbSe NQDs before and after Cl_2 treatment. (a) Cl 2p spectrum. (b) Pb 4f spectrum. (c) Se 3d spectrum. Spectra in (b,c) are vertically shifted for clarity. (d) Schematic illustration of the effect of chlorine treatment on PbSe NQDs.

varying amounts of Cl_2 were added to samples of PbSe NQDs of several sizes. Since the expectation is a surface-based chemical reaction, we adopted a Cl_2 molecule/surface-area normalization for comparison from one experiment to the next, i.e., results are considered in terms of chlorine per unit surface area of PbSe NQDs (Cl_2 concentration in present study varies from 0 to 2 molecules per nm^2), which is calculated from the optically determined NQD size and concentration for a given PbSe NQD dispersion.

Brief exposure to Cl_2 in solution causes a slight blue shift in the absorption and PL spectra of PbSe NQDs, as can be seen in the case of a 6.5 nm diameter sample shown in Figure 1a. For all studied sizes, the degree of shift increases with increasing Cl_2 concentration (Figure 1b) and is generally less pronounced than that produced by Cd-cation exchange.²⁵ The excitonic features in the absorbance spectra and the shape of the PL spectra are retained, although at high treatment concentrations, broadening is observed. This type of systematic blue-shift is consistent with a small decrease in the effective volume of PbSe NQDs, as if by removal of surface atoms, while the increase in PL intensity generally seen in Figure 1c for moderate treatment levels suggests an enhancement in the effectiveness of surface passivation, which is consistent with inorganic shell growth of a higher band gap material by ion exchange instead. Either way, the result is an increase in confinement energy with little effect on optically determined size distribution, except at heavy treatment levels.

Elemental analysis by energy dispersive X-ray spectroscopy (EDX) shows that the Se/Pb atomic ratio of PbSe NQDs

systematically decreases as the Cl_2 concentration increases (Figure 1d), indicating a selective loss of presumably surface Se atoms in preference to Pb atoms even though the NQDs overall were already Pb-rich. Under these oxidative conditions, the Se is likely removed as a mixture of selenium chlorides, including Se_2Cl_2 and SeCl_4 , which is consistent with the observed formation of insoluble orange or yellow products on the vial walls at excessive treatment levels ($\geq 5 \text{ Cl}_2/\text{nm}^2$). X-ray photoelectron spectroscopy (XPS) confirms the presence of Cl with a binding energy similar to Pb-bound Cl²⁷ (Figure 2a). It also shows the emergence of a new feature in the Pb 4f spectrum with a slightly higher binding energy that is also consistent with Pb–Cl bond formation (Figure 2b),²⁸ while the Se 3d spectrum is essentially unchanged (Figure 2c). Finally, we observe no measurable changes to the native oleate ligands by either ¹H nuclear magnetic resonance (NMR) or Fourier-transform infrared absorption (FT-IR) spectroscopies (Figures S3 and S4, respectively).

We can conclude from the above characterization and consideration of standard oxidation/reduction potentials that Cl_2 oxidatively etches surface Se atoms and reacts with surface Pb atoms to form a thin PbCl_x layer, as illustrated in Figure 2d. The process has a negligible effect on the physical sizes of chlorine-treated PbSe NQDs, as determined from HR-TEM images (Figure S5). PbCl_2 has a band gap of $\sim 5 \text{ eV}$ and a calculated valence band position that suggests a type-I alignment with PbS, PbSe, or PbTe.²⁹ Thus, by considering the magnitude of the shift of the PL peak and assuming negligible leakage of excited carriers into a PbCl_x shell, we can

estimate that at treatment levels at which PL QY is highest (generally 1–1.5 Cl_2/nm^2), the thickness of PbCl_x outermost layer is <0.3 nm, which corresponds to ≤ 1 Pb–Cl monolayer (in bulk PbCl_2 , the Pb–Cl bond length is 2.85 Å).

To understand the trend in PL intensity with increasing Cl_2 , we have examined the PL decay dynamics of PbSe NQDs treated with different chlorine concentrations (Figure 3a). At

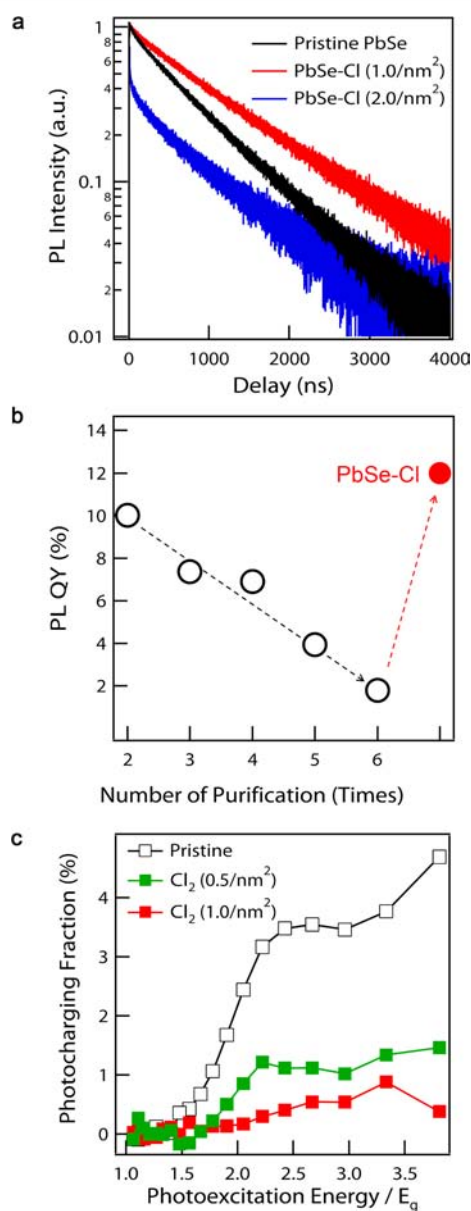


Figure 3. Effect of chlorine treatment on PL decay dynamics and photocharging of PbSe NQDs. (a) PL decay dynamics of 3.9 nm PbSe NQDs with varied chlorine concentrations, showing a slight increase in the PL lifetime for low treatment levels (red) and the onset of a fast decay component at high treatment levels (blue). (b) PL QY of PbSe NQDs as a function of the number of purification steps in the presence of excess oleic acid. PL QY of PbSe NQDs can be regained, and even enhanced, by subsequent chlorine treatment (red). (c) Steady-state photocharging fraction (f_s) in pristine (open squares) and chlorine-treated 3.9 nm PbSe NQDs (solid squares) as a function of pump photon energy normalized by E_g . Suppressed photocharging is observed for Cl_2 -treated PbSe NQDs ($\text{Cl}_2 = 1.0/\text{nm}^2$) at energies above both the first ($\sim 1.5 E_g$) and the second ($\sim 3 E_g$) photocharging thresholds.

moderate treatment levels that yield the highest PL QY, we see a slight increase in PL lifetime, as in the case of the 3.9 nm PbSe NQDs shown in Figure 3a (red trace). This is consistent with a reduction in nonradiative decay mediated by surface trap states presented by surface Se atoms, which are removed through chlorine treatment. However, at heavy treatment levels at which PL QY begins to decline (blue trace), a fast nonradiative decay component (time constant, τ , of ~ 20 ns) emerges. This suggests formation of new trap states, possibly arising at the interface between the PbSe core and a more substantial PbCl_x layer, as the orthorhombic lowest-energy crystal structure of PbCl_2 ($Pnma$, $a = 7.620$, $b = 4.534$, $c = 9.045$ Å)³⁰ is quite different from the rock salt structure of PbSe ($a = b = c = 6.128$ Å).³¹ Alternatively, this could indicate that at high concentrations, chlorine further disrupts the NQD surface either by displacing oleate ligands or by removing Pb atoms, leaving new unpassivated sites. These processes would be consistent with the noted reduction in dispersibility of the most heavily treated NQDs (approaching 10 Cl_2/nm^2), which complicates further analysis by making it extremely difficult to separate the NQDs from other reaction products.

To further test the effect of poorly passivated Se on PL QY, we intentionally removed ligands via repeated purification, which has been shown to lead to trap-state formation.³² We selectively removed trioctylphosphine, which is known to passivate Se atoms,³³ by carrying out each precipitation in the presence of additional excess oleic acid (Figure 3b). As expected, while the oleic acid helps to maintain the redispersibility of the NQDs through interaction with surface Pb atoms, PL QY falls (from 10% down to 1.8%) which can be correlated with an increase in fast trapping (Figure S6). Importantly, PL QY is recovered and even enhanced for the repeatedly purified sample (to 12%) upon Cl_2 treatment, supporting our assertion regarding the role of Se etching and the benefits of Cl passivation.

Surface trap states have also been implicated in the process of photocharging in PbSe NQDs.^{21,22} In photocharging, a “hot” unrelaxed electron or hole in a photoexcited NQD can escape from the nanocrystal, leaving the other carrier in the NQD core. This charge-imbalanced state, which can persist for 10s of seconds, has a large effect on the carrier dynamics because absorption of additional photons effectively creates a three-carrier “trion” state, which can decay by very fast nonradiative Auger recombination instead of by radiative decay. According to recent studies,^{21,22} there can be wide sample-to-sample variation in the average susceptibility of NQDs toward photocharging, ranging from those with nearly zero probability to those where the fraction of “chargeable” NQDs in the ensemble can exceed 10%. This behavior has been attributed to yet unestablished variations in surface structure and passivation arising as a consequence of the colloidal growth method.

Since we show that chlorine treatment consistently improves surface passivation, it could be expected to also affect photocharging. We characterize this effect in terms of the steady-state fraction of photocharged NQDs (degree of photocharging), f_s . Because nonradiative Auger decay of a trion is much faster than its radiative recombination,^{11,22} the photocharged NQDs are essentially nonemissive. As a consequence, the degree of photocharging can be determined from the relative difference of the PL intensity of PbSe NQDs with (I_{PL}) and without sample stirring (I_{PL}^*). In the stirred sample, photocharged NQDs are removed from the excitation volume before they have a chance to absorb a second photon,

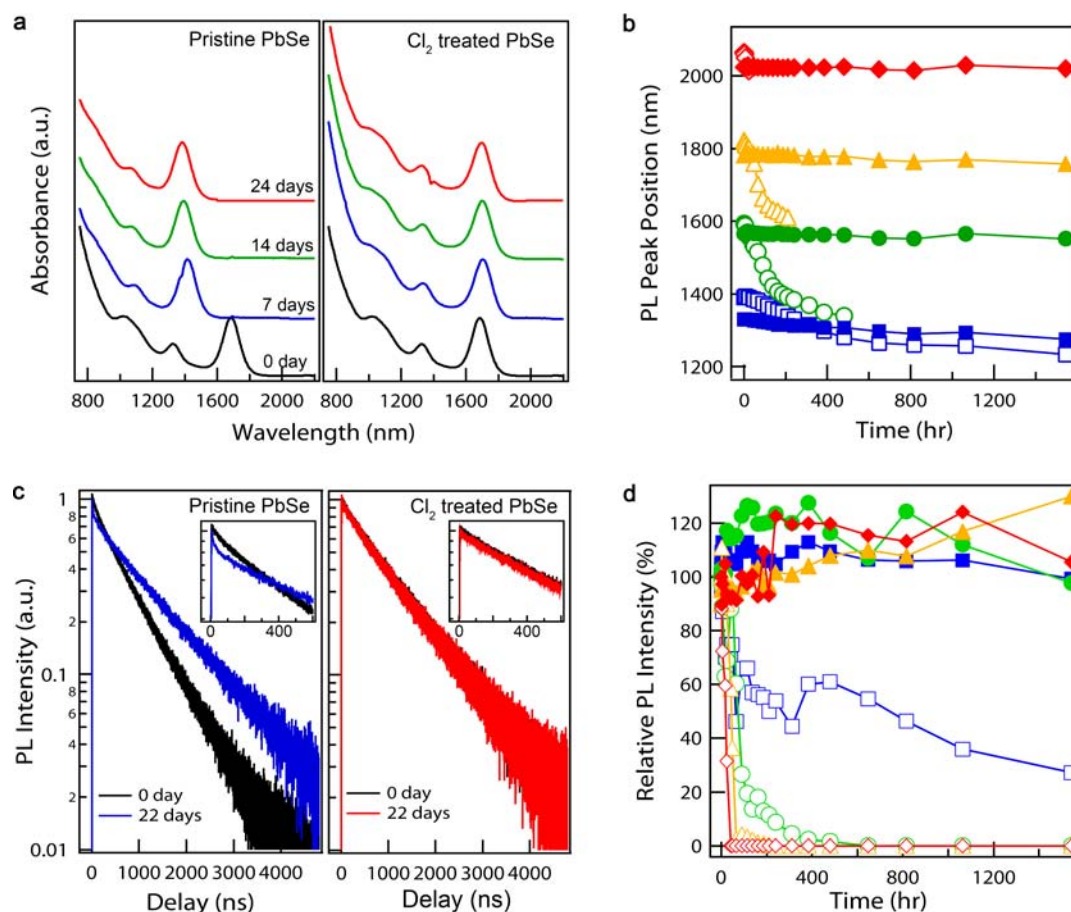


Figure 4. Stability test of PbSe NQDs against oxidation. (a) The evolution of optical absorption spectra of 6.0 nm pristine (left panel) and chlorine-treated PbSe NQDs (right panel) under long-term oxygen exposure. (b) PL peak positions of pristine (open symbols) and chlorine-treated (solid symbols) PbSe NQDs of different sizes (3.9, 5.3, 6.5, and 7.9 nm are average diameters; corresponding data sets are shown by squares, spheres, triangles, and diamonds, respectively) as a function of exposure time in air. Measurements of pristine peak positions stop when these NQDs are no longer emissive. (c) PL decay traces of pristine (left panel) and chlorine-treated (right panel) 5.3 nm PbSe NQDs after 22 days of oxygen exposure. Insets: magnified views of early time dynamics show the emergence of a fast decay component in pristine NQDs after 22 days; this component is absent in the aged Cl₂-treated sample. (d) Relative PL intensities for the samples shown in (b). All samples are treated with Cl₂ concentration of 1.5/nm².

which prevents formation of trions. Without stirring, photocharged NQDs accumulate within the excitation volume, and as a result, the steady-state emission intensity is reduced by a factor of $(1 - f_s)$. Therefore, f_s can be determined from $f_s = 1 - I_{PL}^*/I_{PL}$.^{21,22} As was shown in ref 21, photocharging is characterized by a spectral onset (threshold) that lies above the band gap energy. It was also observed that above this threshold, the degree of photocharging rapidly increases with increasing pump photon energy. A convenient approach to deriving the spectral dependence of f_s is from PL excitation (PLE) measurements on stirred vs static samples.²¹ We use this method here to compare the effect of photocharging in pristine PbSe NQDs to that in the same NQDs after treatment with various concentrations of Cl₂.

Figure 3c shows how the photocharging fraction f as a function of photon energy changes for a typical sample before (black) and after (green and red) treatment. The pristine PbSe NQDs (3.9 nm diameter, emitting at 1330 nm) show a threshold for weak charging at excitation energy of $\sim 1.5 E_g$ and a second threshold at $\sim 3 E_g$, which is consistent with previous reports.²¹ After Cl₂ treatment, the same PbSe NQDs show a significant reduction of the photocharging fraction at both thresholds, again indicating that passivation has been

significantly improved. Importantly, photocharging suppression is typically most effective at treatment levels that also yield the highest PL QY enhancements, suggesting that Se trap sites affect both processes.

The removal of surface Se atoms accompanied by the formation of the thin PbCl_x passivation layer not only enhances PL QY of PbSe NQDs but also significantly improves the spectral stability of PbSe NQDs over time under ambient conditions (Figure 4). As is well established, pristine PbSe NQDs are prone to large blue-shifts in optical absorption and PL spectra over time (Figure 4a, left panel and 4b, open symbols) as a result of oxidation processes^{18,33} that also open a fast nonradiative decay channel (Figure 4c, left panel) and concomitant reduction of PL QY (Figure 4d, open symbols). Larger PbSe NQDs are particularly susceptible to oxidation as compared with smaller PbSe NQDs: 7.9 nm NQDs with emission at 2090 nm lost essentially all PL within 20 h, while 3.9 nm NQDs retained roughly 30% of their original emission even after 1500 h. In contrast to pristine PbSe NQDs, Cl₂-treated PbSe NQDs of all sizes generally preserve their optical properties under long-term air exposure (Figure 4a, right panel and 4b, solid symbols). This is consistent with previous observation of the presence of SeO_x species in aged or poorly

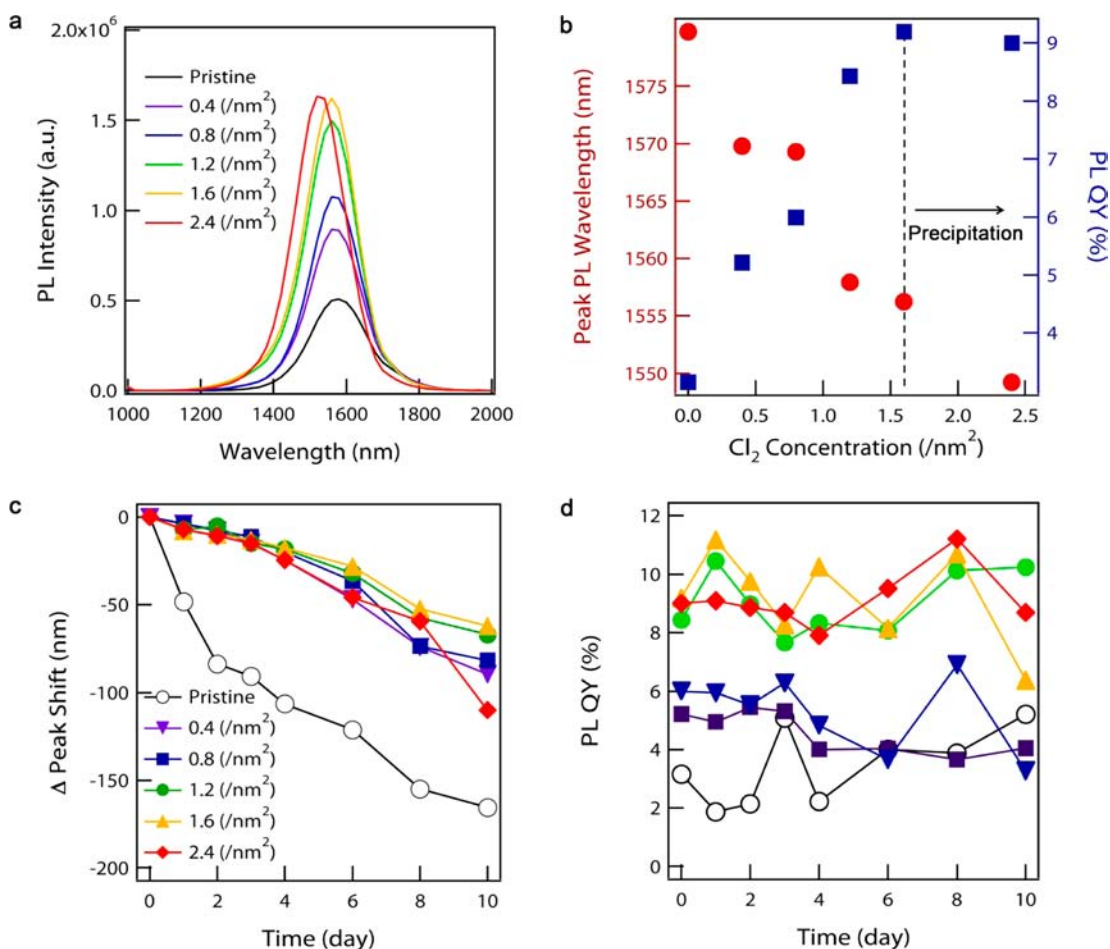


Figure 5. Chlorine treatment of PbS NQDs ($d = 6$ nm). (a) PL spectra of PbS NQDs as a function of Cl_2 concentration. A slight blue-shift is observed at the highest treatment levels as a result of surface etching of PbS NQDs by Cl_2 . (b) Peak PL wavelength (left) and PL QYs (right) of PbS NQDs treated with different amounts of Cl_2 . We denote that the treatment with high concentration of chlorine results in the precipitation of some PbS NQDs possibly due to the removal of oleate ligands. (c,d) Spectral shift of the 1S absorption peak (c) and the relative PL intensity (d) of PbS NQDs treated with different amounts of Cl_2 during prolonged exposure to the air.

passivated PbSe NQDs³⁴ that implies surface Se sites are responsible for sensitivity toward oxidation. However, it is worth noting that unlike the case for PL QY, there does not seem to be an optimal Cl_2 concentration (i.e., $\sim 1\text{--}1.5/\text{nm}^2$) for greatest stability enhancement: stability is generally as good or better as Cl_2 concentration increases up until the point at which complete loss of PL makes spectral stability measurement impossible (Figure S7). This is reminiscent of similar reports that while increasingly thick inorganic passivation shells can enhance the chemical stability of NQD cores, this can be accompanied by an increase in the number of interfacial defects due to the structural difference (i.e., lattice mismatch) between core and shell materials, leading to a decrease in PL QY.³⁵ Therefore, one may need to use a balance of these considerations to adjust the Cl_2 concentration depending on whether the desired application requires optimal PL QY or the most rigorous stability. Finally, similar tests of drop-cast NQD films indicate that, importantly, this enhanced stability extends to solid PbSe NQD arrays as well (Figure S9).

The methodology described in the present work is distinct from simple ligand exchange methods, such as those applied to NQD films for enhancement of device properties, in that active Cl_2 actually reacts with the surface of PbSe NQDs to remove surface Se atoms and to form thin PbCl_x layers rather than

simply replacing surface-bound ligands. In this respect, it is probably better compared to the previously reported Cd treatments of lead chalcogenide NQDs.²⁵ In either method, both PL enhancement and long-term stability can be achieved via a relatively fast, low-temperature process compatible with conventional solution-based processing methods. However, by using Cl_2 , these enhancements are achieved with a submonolayer shell of PbCl_x which should not hamper either carrier extraction or carrier transport between NQDs in a solid film, which is a potential drawback of the $1\text{--}1.5$ nm thick CdSe shell typical of stable Cd-treated PbSe NQDs. Thus, this new method could prove highly preferable for solution-processed (e.g., spin-cast or dip-coated)^{3,13,16,17,36–42} films for use in optoelectronic devices.

This methodology is inherently flexible and useful not only for a range of PbSe NQD sizes but also effective for PbSe NQDs prepared using 1,2-hexadecanediol reducing agent (Figure S8).⁴³ Further, we have found it can be applied to PbS NQDs as well, even though these are generally considered to be more stable than PbSe NQDs. In Figure 5a,b, we see that initial exposure of PbS NQDs (6.0 nm diameter, emitting at 1590 nm) to Cl_2 solutions at a similar range of concentrations produces familiar effects, including PL QY enhancement accompanied by slight spectral blue shift, suggesting a similar

etching mechanism. In this case, we are not able to determine whether this enhancement has an upper concentration threshold, as at concentrations >1.5 Cl/nm², the NQDs start to precipitate from dispersion. As expected, these large pristine PbS NQDs fare much better than PbSe NQDs over long-term exposure to air (Figure 5c,d); however, all Cl-treated NQDs still show noticeably improved QY and peak shift stability. Results are slightly less dramatic than those for PbSe NQDs, which we attribute to a lower overall reactivity of surface S atoms toward Cl₂ that possibly allows increased contributions from deleterious processes (loss of ligand and surface Pb). Preliminary studies on treatment of PbTe NQDs synthesized by literature methods⁸ are much less consistent: Spectral stability can be enhanced on the short-term (<1 day), but the reactivity of PbTe NQDs toward Cl₂ seems much faster and less self-limiting, leading to substantial precipitation and even decomposition of the NQDs even at modest concentrations. Overall, our observed reactivity trend is consistent with the trend in oxidation potentials of the chalcogenide ions themselves ($S^{2-} < Se^{2-} < Te^{2-}$).

CONCLUSIONS

We have presented a facile chemical means to improve the optical properties and enhance stability toward oxidation of PbSe NQDs. It is based on the reaction of small amounts of Cl₂ in dilute solution phase at room temperature to preferentially etch out surface Se atoms and react with surface Pb atoms to form a thin PbCl_x layer. The resulting NQDs show strikingly increased stability in solution as well as in films and show both enhanced PL QY and reduced photocharging.

Importantly, these results implicate surface Se atoms as having a large role in the type of carrier trapping events responsible for both loss of PL QY and photocharging as well as in the reaction of PbSe NQDs with oxygen under ambient conditions. In comparing studies of other lead chalcogenides, we find that the trend in susceptibility of NQDs toward air-oxidation (PbS < PbSe < PbTe, as manifested in their spectral stability under ambient conditions) as well as toward reaction with Cl₂ can be explained in terms of the oxidation potential of each respective chalcogenide ion. Finally, we note that due to the simplicity of this procedure and the relatively small perturbation of the total structure of the treated NQDs, both the method and the product NQDs are highly compatible with use in solution-processed optoelectronic applications, particularly for next-generation photovoltaics.

EXPERIMENTAL METHODS

General Considerations. All NQD syntheses were performed under exclusion of air and moisture using standard Schlenk or inert-atmosphere glovebox techniques until after reaction with Cl₂. Preparation of the Cl₂ stock solution was performed in a chemical fume hood, and handling of dilute solutions was performed in an inert-atmosphere glovebox. Lead(II) oxide (PbO, Alfa Aesar, 99.999%), selenium powder (Aldrich, 99.999%), oleic acid (OA, Aldrich, 90%), trioctylphosphine (TOP, Strem, 97%), 1-octadecene (ODE, Aldrich, 90%), and bis(trimethylsilyl)sulfide (Acros, 98%), di-isobutylphosphine (Strem, min. 93%), aqueous hydrochloric acid (37.5%, Fisher), aqueous sodium hypochlorite (4–6%, Fisher), and anhydrous calcium chloride (CaCl₂, flake, Fisher) were used without further purification. A 2 M TOPSe stock solution was prepared by stirring the appropriate amount of Se powder in TOP overnight at ~120 °C in an inert atmosphere glovebox. Absorption and PL spectra were collected on dispersions of NQDs in “extra dry” tetrachloroethylene (after

synthesis, Acros, 99%) or toluene (during stability study, Acros, 99.8%).

Synthesis of PbSe NQDs. PbSe NQDs were prepared in a manner similar to previously reported methods.²⁵ In a typical synthesis, 0.6 g of PbO, 6 mL of OA, 8 mL of TOP, and 8 mL of ODE were loaded into a 100 mL round-bottom flask. The flask was degassed under vacuum at 110 °C for 1 h to form a colorless solution of Pb(oleate)₂ complex, which was then heated to the desired injection temperature (typically 170–210 °C). Four ml of 2 M TOPSe containing a varied amount of di-isobutylphosphine (0.05–0.4 mL) was swiftly injected into the flask with stirring, and the reaction temperature was maintained until the desired size of PbSe NQDs were synthesized (typically 5–120 s). PbSe NQDs described as having been prepared using 1,2-hexadecanediol as a reducing agent were synthesized according to the method of a previous report.⁴³ All samples were purified twice by precipitation with 10 mL of ethanol, centrifugation, decanting of the supernatant, and redispersion to remove residual precursors and excess ligands. Samples were stored in toluene under Ar atmosphere previous to Cl₂ treatment and/or oxidation stability studies.

Synthesis of PbS NQDs. The synthesis of PbS NQDs was adapted from a literature report.⁷ For 6 nm diameter PbS NQDs, 0.11 g of PbO, 0.5 mL of OA, and 10 mL of ODE were loaded into a 100 mL round-bottom flask, degassed at 110 °C for 1h, and then heated to 210 °C. Two ml of ODE containing 0.04 mL of bis(trimethylsilyl)sulfide was swiftly injected into the flask with stirring, and the reaction was then allowed to come to room temperature. Purification and handling were carried out in the same manner as above for PbSe NQDs.

Chlorine treatment. Cl₂-containing solution was prepared by bubbling the gas released from the reaction of aqueous hydrochloric acid and sodium hypochlorite (6 wt % in water), dried by passing over anhydrous CaCl₂, through CCl₄ at room temperature under an Ar atmosphere. The Cl₂ concentration in fresh solution was measured by iodometry to be 0.16 M; this was then diluted to create a 10 mM stock solution. Chlorine treatment of PbSe NQDs was carried out in solution phase at room temperature. One ml of PbSe NQDs dispersed in toluene (1 mM) was mixed with an appropriate volume of Cl₂ stock solution. After 1 min, the treated NQDs were purified by precipitation via addition of polar solvent (EtOH or MeOH/acetone mixture), centrifugation, decanting of the supernatant, and redispersion in nonpolar organic solvent. PbS NQDs were treated in a very similar manner. The chlorine concentration per unit surface area of PbSe NQDs was calculated from the amount of Cl₂ solution, the optically determined concentration of PbSe NQD dispersion, and the calculated NQD surface area based on the optically determined average diameter.⁴⁴ NQD concentrations, n_{NQD} , were determined via a previously reported method⁴³ from the OD at 400 nm of sample dispersions using the expression $n_{\text{NQD}} = \text{OD} \ln(10)/\sigma_a$, where σ_a is an NQD absorption cross section at 400 nm. Absorption cross sections were calculated based on the bulk PbSe absorption coefficient, α_0 , scaled by the NQD volume, V_0 , and the local-field correction factor, η ,⁴⁵ according to the expression $\sigma_a = \alpha_0(n_b/n_{\text{sol}})V_0|\eta|^2$, in which n_b and n_{sol} are the refractive indices of bulk PbSe and the solvent, respectively. This method for optically determining NQD concentration was verified to yield values in good agreement with those determined by more direct measurements involving elemental analysis.⁴⁴

Stability test against oxidation. PbSe NQDs dispersed in toluene (typically 0.1 mM) were exposed to air under room light by vigorous stirring in 20 mL sample vials left uncapped. Aliquots taken to characterize optical properties of PbSe NQDs during oxidation were replaced after being measured. Periodically, appropriate amounts of solvent were added to the test sample to replace evaporative losses.

Spectroscopic studies. Absorption spectroscopy was performed on PbSe NQD dispersions in tetrachloroethylene using a Perkin-Elmer Lambda 1050 spectrophotometer. Steady-state and time-resolved PL measurements were performed on toluene dispersions of NQDs. In steady-state measurements, the mechanically chopped light from an 808 nm diode laser was used to excite the NQDs, and PL spectra were collected using a grating monochromator and a liquid N₂-chilled InSb detector using lock-in amplification to discard background. PL QYs of

as-synthesized NQDs were determined relative to IR-26 dye, assuming a dye QY of 0.048%, with an estimated error of 0.002%;⁴⁶ since this uncertainty is larger than the error from the individual measurement of PL intensities, all of our reported QYs can be assumed to have an error of 4% of the reported value. All QYs during aging studies were determined by comparing intensities to those of the initial as-synthesized sample, using dispersions of identical optical density. Time-resolved PL spectroscopy was performed using a Hamamatsu H10330A infrared photomultiplier tube with InP/InGaAs photocathode, on samples excited with 800 nm light (pulse width <2 ps, repetition rate 10 kHz) from an amplified Ti-sapphire laser. Photocharging measurements were performed as previously described²¹ on dispersions of NQDs in toluene.

■ ASSOCIATED CONTENT

■ Supporting Information

Absorption and PL spectra of pristine PbSe NQDs; IR and NMR spectra; high-resolution transmission electron microscopy images before and after Cl₂ exposure, with EDX elemental analysis; static and transient spectral data from purification studies; spectral stability studies of PbSe NQD films. This material is available free of charge via the Internet at <http://pubs.acs.org>.

■ AUTHOR INFORMATION

Corresponding Author

pietryga@lanl.gov; klimov@lanl.gov

Author Contributions

^{||}These authors contributed equally.

Notes

The authors declare no competing financial interest.

■ ACKNOWLEDGMENTS

This material is based upon work within the Center for Advanced Solar Photophysics (CASP), an Energy Frontier Research Center funded by the U.S. Department of Energy (DOE), Office of Science, Office of Basic Energy Sciences (BES). D.C.L. was a CASP member supported by a Los Alamos National Laboratory Director's Fellowship. Q.L. and H.L. are CASP affiliates supported by the New Mexico Consortium and Los Alamos National Laboratory.

■ REFERENCES

- (1) Sun, L.; Choi, J. J.; Stachnik, D.; Bartnik, A. C.; Hyun, B.-R.; Malliaras, G. G.; Hanrath, T.; Wise, F. W. *Nat. Nanotechnol.* **2012**, *7*, 369.
- (2) Schaller, R. D.; Petruska, M. A.; Klimov, V. I. *J. Phys. Chem. B* **2003**, *107*, 13765.
- (3) Konstantatos, G.; Howard, I.; Fischer, A.; Hoogland, S.; Clifford, J.; Klem, E.; Levina, L.; Sargent, E. H. *Nature* **2006**, *442*, 180.
- (4) Murray, C. B.; Sun, S. H.; Gaschler, W.; Doyle, H.; Betley, T. A.; Kagan, C. R. *IBM J. Res. Dev.* **2001**, *45*, 47.
- (5) Rogach, A. L.; Eychmüller, A.; Hickey, S. G.; Kershaw, S. V. *Small* **2007**, *3*, 536.
- (6) Pietryga, J. M.; Schaller, R. D.; Werder, D.; Stewart, M. H.; Klimov, V. I.; Hollingsworth, J. A. *J. Am. Chem. Soc.* **2004**, *126*, 11752.
- (7) Hines, M. A.; Scholes, G. D. *Adv. Mater.* **2003**, *15*, 1844.
- (8) Murphy, J. E.; Beard, M. C.; Norman, A. G.; Ahrenkiel, S. P.; Johnson, J. C.; Yu, P.; Micić, O. I.; Ellingson, R. J.; Nozik, A. J. *J. Am. Chem. Soc.* **2006**, *128*, 3241.
- (9) Evans, C. M.; Guo, L.; Peterson, J. J.; Maccagnano-Zacher, S.; Krauss, T. D. *Nano Lett.* **2008**, *8*, 2896.
- (10) Schaller, R. D.; Klimov, V. I. *Phys. Rev. Lett.* **2004**, *92*, 186601.
- (11) McGuire, J. A.; Sykora, M.; Joo, J.; Pietryga, J. M.; Klimov, V. I. *Nano Lett.* **2010**, *10*, 2049.

- (12) Ellingson, R. J.; Beard, M. C.; Johnson, J. C.; Yu, P.; Micić, O. I.; Nozik, A. J.; Shabaev, A.; Efros, A. L. *Nano Lett.* **2005**, *5*, 865.
- (13) Semonin, O. E.; Luther, J. M.; Choi, S.; Chen, H.-Y.; Gao, J.; Nozik, A. J.; Beard, M. C. *Science* **2011**, *334*, 1530.
- (14) Luther, J. M.; Gao, J.; Lloyd, M. T.; Semonin, O. E.; Beard, M. C.; Nozik, A. J. *Adv. Mater.* **2010**, *22*, 3704.
- (15) Gao, J.; Perkins, C. L.; Luther, J. M.; Hanna, M. C.; Chen, H.-Y.; Semonin, O. E.; Nozik, A. J.; Ellingson, R. J.; Beard, M. C. *Nano Lett.* **2011**, *11*, 3263.
- (16) Tang, J.; Kemp, K. W.; Hoogland, S.; Jeong, K. S.; Liu, H.; Levina, L.; Furukawa, M.; Wang, X.; Debnath, R.; Cha, D.; Chou, K. W.; Fischer, A.; Amassian, A.; Asbury, J. B.; Sargent, E. H. *Nat. Mater.* **2011**, *10*, 765.
- (17) Ip, A. H.; Thon, S. M.; Hoogland, S.; Voznyy, O.; Zhitomirsky, D.; Debnath, R.; Levina, L.; Rollny, L. R.; Carey, G. H.; Fischer, A.; Kemp, K. W.; Kramer, I. J.; Ning, Z.; Labelle, A. J.; Chou, K. W.; Amassian, A.; Sargent, E. H. *Nat. Nanotechnol.* **2012**, *7*, 577.
- (18) Sykora, M.; Kaposov, A. Y.; McGuire, J. A.; Schulze, R. K.; Tretiak, O.; Pietryga, J. M.; Klimov, V. I. *ACS Nano* **2010**, *4*, 2021.
- (19) Stewart, J. T.; Padilha, L. A.; Qazilbash, M. M.; Pietryga, J. M.; Midgett, A. G.; Luther, J. M.; Beard, M. C.; Nozik, A. J.; Klimov, V. I. *Nano Lett.* **2011**, *12*, 622.
- (20) Nagpal, P.; Klimov, V. I. *Nat. Commun.* **2011**, *2*, 486.
- (21) Padilha, L. A.; Robel, I.; Lee, D. C.; Nagpal, P.; Pietryga, J. M.; Klimov, V. I. *ACS Nano* **2011**, *5*, 5045.
- (22) McGuire, J. A.; Sykora, M.; Robel, I.; Padilha, L. A.; Joo, J.; Pietryga, J. M.; Klimov, V. I. *ACS Nano* **2010**, *4*, 6087.
- (23) Gaponik, N.; Hickey, S. G.; Dorfs, D.; Rogach, A. L.; Eychmüller, A. *Small* **2010**, *6*, 1364.
- (24) Lee, D. C.; Robel, I.; Pietryga, J. M.; Klimov, V. I. *J. Am. Chem. Soc.* **2010**, *132*, 9960.
- (25) Pietryga, J. M.; Werder, D. J.; Williams, D. J.; Casson, J. L.; Schaller, R. D.; Klimov, V. I.; Hollingsworth, J. A. *J. Am. Chem. Soc.* **2008**, *130*, 4879.
- (26) Liu, Y.; Gibbs, M.; Perkins, C. L.; Tolentino, J.; Zarghami, M. H.; Bustamante, J.; Law, M. *Nano Lett.* **2011**, *11*, 5349.
- (27) Blake, P. G.; Carley, A. F.; Di Castro, V.; Roberts, M. W. *J. Chem. Soc., Faraday Trans. 1* **1986**, *82*, 723.
- (28) Pederson, L. R. *J. Electron Spectrosc. Relat. Phenom.* **1982**, *28*, 203.
- (29) Ahmed, G.; Sharma, Y.; Ahuja, B. L. *Appl. Radiat. Isot.* **2009**, *67*, 1050.
- (30) Sass, R. L.; Brackett, E. B.; Brackett, T. E. *J. Phys. Chem.* **1963**, *67*, 2863.
- (31) Noda, Y.; Ohba, S.; Sato, S.; Saito, Y. *Acta Crystallogr., Sect. B: Struct. Sci.* **1983**, *39*, 312.
- (32) Bolotin, I. L.; Asunskis, D. J.; Jawaid, A. M.; Liu, Y.; Snee, P. T.; Hanley, L. J. *J. Phys. Chem. C* **2010**, *114*, 16257.
- (33) Moreels, I.; Fritzing, B.; Martins, J. C.; Hens, Z. *J. Am. Chem. Soc.* **2008**, *130*, 15081.
- (34) Sapra, S.; Nanda, J.; Pietryga, J. M.; Hollingsworth, J. A.; Sarma, D. D. *J. Phys. Chem. B* **2006**, *110*, 15244.
- (35) Dabbousi, B. O.; Rodriguez-Viejo, J.; Mikulec, F. V.; Heine, J. R.; Mattoussi, H.; Ober, R.; Jensen, K. F.; Bawendi, M. G. *J. Phys. Chem. B* **1997**, *101*, 9463.
- (36) Talapin, D. V.; Murray, C. B. *Science* **2005**, *310*, 86.
- (37) Zarghami, M. H.; Liu, Y.; Gibbs, M.; Gebremichael, E.; Webster, C.; Law, M. *ACS Nano* **2010**, *4*, 2475.
- (38) Beard, M. C.; Midgett, A. G.; Law, M.; Semonin, O. E.; Ellingson, R. J.; Nozik, A. J. *Nano Lett.* **2009**, *9*, 836.
- (39) Luther, J. M.; Law, M.; Song, Q.; Perkins, C. L.; Beard, M. C.; Nozik, A. J. *ACS Nano* **2008**, *2*, 271.
- (40) Luther, J. M.; Beard, M. C.; Song, Q.; Law, M.; Ellingson, R. J.; Nozik, A. J. *Nano Lett.* **2007**, *7*, 1779.
- (41) Sukhovatkin, V.; Hinds, S.; Brzozowski, L.; Sargent, E. H. *Science* **2009**, *324*, 1542.
- (42) Clifford, J. P.; Konstantatos, G.; Johnston, K. W.; Hoogland, S.; Levina, L.; Sargent, E. H. *Nat. Nanotechnol.* **2009**, *4*, 40.

(43) Joo, J.; Pietryga, J. M.; McGuire, J. A.; Jeon, S.-H.; Williams, D. J.; Wang, H.-L.; Klimov, V. I. *J. Am. Chem. Soc.* **2009**, *131*, 10620.

(44) Moreels, I.; Lambert, K.; De Muynck, D.; Vanhaecke, F.; Poelman, D.; Martins, J. C.; Allan, G.; Hens, Z. *Chem. Mater.* **2007**, *19*, 6101.

(45) Klimov, V. I. *J. Phys. Chem. B* **2000**, *104*, 6112.

(46) Semonin, O. E.; Johnson, J. C.; Luther, J. M.; Midgett, A. G.; Nozik, A. J.; Beard, M. C. *J. Phys. Chem. Lett.* **2010**, *1*, 2445.